Repurposing HIV antiretroviral drug efavirenz against chikungunya virus.

Sanketkumar Nehul[1], Ruchi Rani[1], Shailly Tomar[1]*

[1]Department of Biosciences and Bioengineering, Indian Institute of Technology Roorkee, Uttarakhand (247667), India

***Corresponding author details**

Shailly Tomar*

Professor,
Department of Biosciences and Bioengineering,
Indian Institute of Technology Roorkee,
Uttarakhand, India 247667
Tel: +91-1332-285849
Fax: 91-1332-273560
Email: shailly.tomar@bt.iitr.ac.in
ORCID ID: 0000-0002-1730-003X

Abstract

Chikungunya virus (CHIKV) is frequently recurring in recent decades, causing outbreaks worldwide in tropical and subtropical regions. The re-emergence of CHIKV poses a substantial risk to human health as no efficacious medical countermeasures are available to curb new outbreaks effectively. The interaction of the cytoplasmic domain of E2 (cdE2) with the conserved hydrophobic pocket of capsid protein (CP) is crucial for virus budding. Here, we identified efavirenz molecular interactions with the CP (K_D = 6.22 µM), making it a potential antiviral candidate against CHIKV as it is expected to disrupt the cdE2-CP interaction. Subsequently, anti-CHIKV activity of efavirenz by an *in-vitro* cell based antiviral assay, immunofluorescence assay (IFA), and quantitative reverse transcription polymerase chain reaction (qRT-PCR) was investigated. These studies demonstrated dose-dependent robust anti-CHIKV activity of efavirenz at low micromolar concentration (EC_{50} = 1.33 µM). To demonstrate broad anti-alphavirus activity of efavirenz, its inhibitory activity against Sindbis virus (SINV) was detected. Interestingly, efavirenz also inhibited the replication of SINV at low micromolar range (EC_{50} = 0.7 µM). Efavirenz is the a non-nucleoside reverse transcriptase inhibitor (NNRTI) used to treat acquired immunodeficiency syndrome (AIDS) and it it has good oral bioavailability, long half-life and affordable low cost. Collectively, the present study emphasize the repurposing of efavirenz as an antiviral treatment against CHIKV infection and to curb CHIKV outbreaks in the initial phase.

Introduction

Chikungunya virus (CHIKV) is a re-emerging mosquito-transmitted alphavirus from the family *Togaviridae*, was first reported in Tanzania between 1952-1953 in the serum sample of a febrile patient (Robinson, 1955). CHIKV is an etiological agent of chikungunya fever characterized by polyarthralgia, headache, maculopapular rash, and asthenia (Bodenmann & Genton, 2006; Pialoux et al., 2007). CHIKV-infected patients experience chronic joint and musculoskeletal pain that might last months to years after post-acute infection, causing considerable suffering and economic loss (Suhrbier, 2019). From an epidemiological and medical perspective, CHIKV is the most prevalent alphavirus transmitted to humans by *Aedes albopictus* and *Aedes aegypti*. One hundred and fourteen countries over sub-tropical and tropical regions of Asia, Africa, Europe, and the Americas have reported autochthonous transmission of CHIKV (Puntasecca et al., 2021).

Earlier, the CHIKV outbreaks were limited to Sub-Saharan Africa (Powers & Logue, 2007); then, in 2004, the East/Central/South African (ECSA) strain re-emerged in Kenya (Chretien et al., 2007). The ECSA strain underwent rapid evolution and transmitted to new regions of islands in the Indian Ocean, India, and certain parts of Southeast Asia, resulting in an estimated 6 million cases (Erin Staples et al., 2009; Powers & Logue, 2007). Within the clade ECSA, the Indian Ocean Lineage (IOL) displayed an alanine (Ala or A) to valine (Val or V) substitution mutation in the E1 glycoprotein at position 226. This adaptive mutation increased the transmission rate by 40-fold via the vector *Aedes albopictus* while not affecting viral fitness in the *A. aegypti* vector (Tsetsarkin et al., 2007; Volk et al., 2011). In addition to the mutation in CHIKV, the dense human population due to unplanned urban growth and modern rapid transportation has increased the risk of outbreaks (Ryan et al., 2018). Another major outbreak occurred in December 2013, when a strain from the Asian lineage emerged on

Saint Martin Island in the Caribbean Sea (Cassadou et al., 2014). Thus, to counter large-scale epidemics of CHIKV with high attack rates, there is an imminent need to develop effective therapeutics for outbreak containment.

Despite the threat to global human health, no efficacious medical countermeasures are available against CHIKV. As a result, the treatment primarily relies on symptom management using anti-inflammatory and analgesic drugs such as paracetamol to alleviate the symptoms (Abdelnabi et al., 2015). However, targeting various structural and non-structural proteins (nsPs) of CHIKV presents a promising avenue for finding effective drugs, as these viral proteins play a vital role in the replication cycle of virus. Structural and nsPs have been targeted in different studies to discover potent drug molecules. However, effective drug treatment molecules or vaccine development is unsuccessful (Kovacikova & van Hemert, 2020). Additionally, repurposing drugs already in clinical use for other diseases to target CHIKV viral proteins can offer a valuable strategy, potentially avoiding the need for the time-consuming and expensive drug trials of novel compounds (Pushpakom et al., 2018).

CHIKV is a positive-sense enveloped RNA virus with a 5´-capped and 3´-polyadenylated genomic of ~11.8 kb. The CHIKV genome comprises two open reading frames (ORFs), of which the 5´ ORF codes for a CHIKV nsP that is translated and cleaved in four nsPs (nsP1,2,3,4) (Khan et al., 2002; Solignat et al., 2009). The other 3´ ORF transcribes a sub-genomic positive-stranded RNA that encodes structural proteins (CP, E1, E2, E3, and 6K). These structural proteins play essential roles at different stages of the CHIKV life cycle. E1, E2, and E3 are involved in receptor recognition, binding, and fusion processes (Voss et al., 2010), while the nucleocapsid facilitates genome encapsidation and virus budding (Kim et al., 2005; Lee et al., 1996), and 6K protein forms the cation-selective ion channels (Melton et al., 2002; Sanz et al., 2003).

Structural proteins play a vital role in forming mature CHIKV virion particles. The mature virion encompasses two concentric shells comprising 240 copies of each capsid, E1, and E2 proteins. The inner shell comprises capsid protein (CP), while the outer shell consists of E1 and E2 glycoproteins (Holland Cheng et al., 1995; Strauss & Strauss, 1994). The lipid bilayer derived from the host cell occupies the space between two concentric shells. The transmembrane helix of the glycoproteins penetrates through the host-derived lipid bilayer (Mancini et al., 2000; Tang et al., 2011). Crystallographic and cryo-electron microscopy studies of different alphaviruses unravel information about the distribution, structures, and possible interactions of the cytoplasmic tail of E1 and E2 glycoproteins with CP (Kostyuchenko et al., 2011; W. Zhang et al., 2002). The protein-protein interaction (PPI) of the hydrophobic pocket of CP with the cdE2 enables the maturation, budding and release of virions from the plasma membrane of the infected host cell (Jose et al., 2012).

The crystal structure of Sindbis virus (SINV) CP revealed the presence of solvent-derived dioxane in its hydrophobic pocket (Lee et al., 1998), suggesting that the small molecules could access the pocket and potentially hinder CP–cdE2 binding. Leveraging this information, dioxane-based synthetic antiviral compounds have been designed to target and disrupt CP-cdE2 interaction against the crystal structure of SINV CP-containing dioxane in the hydrophobic pocket (Kim et al., 2005, 2007). Similarly, in the case of CHIKV, the hydrophobic pocket can be targeted to disrupt the interaction between cdE2 and CP to inhibit CHIKV replication. The hydrophobic pocket is conserved in the CP of different alphaviruses (Aggarwal et al., 2017; Sharma et al., 2016, 2018). Thus, the hydrophobic pocket is a potential target for developing effective antivirals against alphaviruses, including CHIKV, by interfering with their maturation and budding process.

The present study employed computational-assisted virtual screening of the Selleckchem library to specifically target CP's hydrophobic pocket. The screening identified top-hit compounds, of which four jervine, efavirenz, dehydrocholic acid, and tomatidine were shortlisted based on their favourable pharmacokinetic properties. Among the four studied compounds, efavirenz exhibited a significant affinity towards CP, as evidenced by surface plasmon resonance (SPR). Subsequently, an *in-vitro* cell culture-based assay demonstrated a concentration-dependent reduction in extracellular infectious virus particle production upon treatment with efavirenz. In accordance with plaque assay results, a drastic reduction in number of infected cells as compared to virus control upon compound treatment was observed by immunofluorescence assay (IFA). A significant reduction in intracellular viral RNA was observed after efavirenz treatment as compared to virus control, further corroborating efavirenz's potential as an anti-CHIKV compound. Broad spectrum anti-alphavirus activity of efavirenz was validated by detecting the anti-sindbis (SINV) activity of efavirenz. Time of compound addition assay proved that efavirenz is most effective in the post-treatment of infected cells, indicating that efavirenz is acting at later stages of virus replication. Efavirenz is the first-generation non-nucleoside reverse transcriptase inhibitor (NNRTI) used to treat acquired immunodeficiency syndrome (AIDS). Interestingly, efavirenz binds to the hydrophobic region of HIV-1 reverse transcriptase (RT) (Maggiolo, 2007). Based on good pharmacokinetics properties, previous successful application of efavirenz to treat HIV infection and demonstration of robust anti-CHIKV activity of efavirenz in the present study, indicates great potential to repurpose efavirenz against CHIKV infection.

Materials and methods

Virtual library screening targeting hydrophobic pocket of Capsid protein

The structural information for CP was retrieved from the Protein Data Bank (PDB) database with the associated PDB ID: 5H23 (Sharma et al., 2018). The structure was downloaded in .pdb format. Subsequently, a screening of the Selleckchem library containing 2370 compounds against the hydrophobic pocket of CP was performed, and the compounds were retrieved in .sdf format. The entire screening process, from the refinement of protein and ligands to virtual screening, was followed as previously described (Rani et al., 2022), using the macOS Mojave workstation.

For comparison, the binding energies (B.E.) of virtual screened compounds were compared with the cdE2 peptide (Thr398 - Val408). The residues of cdE2 (Thr398 – Val408) were selected based on the interacting region of cdE2 with the hydrophobic pocket from the Cryo-EM structure of the CHIKV (PDB ID : 7CVY). The peptide was designed using ChemDraw (Brown, 2014) to dock against the hydrophobic pocket. Subsequently, compounds with B.E. ≥8 kcal/mol were selected based on their drug-likeness properties. Compound pharmacokinetic properties and toxicity are vital criteria for evaluating the potential of any compound as a drug candidate. SwissADME online tool was utilized to assess the drug-likeness and predict the brain penetration and gastrointestinal absorption of selected compounds (Daina et al., 2017; Daina & Zoete, 2016). With the help of the SwissADME online tool, these properties of screened compounds were assessed as previously described (Rani et al., 2022).

In silico molecular docking

Molecular re-docking was conducted to gain further insights following the *in-silico* drug-likeness study of selected compounds against CP. The AutoDock Vina algorithm was employed for detailed analysis. Molecular docking utilized specific parameters, with the grid

center points, was set at X = 45, Y = 40, and Z = 42, and box dimensions set as -2.333 Å × 10.722 Å × -3.667 Å with an exhaustiveness 8.

The molecular interaction between the compounds and the CP was visualized and analyzed using LIGPLOT^{+}, which visually represents hydrogen (H) and hydrophobic bonds in protein-ligand interactions (Wallace et al., 1995).

Expression and purification of Capsid Protein

The CP was expressed and purified as previously described (Sharma et al., 2016). The recombinant construct pET28c containing the CP gene and N-terminal 6X-his-tag was transformed into *Escherichia coli* (Rosetta) and was grown overnight at 37 ºC in 10 mL of Luria Broth (LB) supplemented with chloramphenicol (35 µg/mL) and kanamycin (50 µg/mL). The primary culture was utilized to raise the secondary culture. When the OD_{600} was around 0.6, the culture was induced with 0.4 mM isopropyl-β-D-1-thiogalactopyranoside (IPTG) and further incubated for five h at 37 °C with continuous shaking at 180 rpm. Post incubation, the culture was harvested by centrifugation.

For purification, the culture pellet was resuspended in 50 mL lysis buffer containing 50 mM Tris-HCl (pH 7.6), 100 mM NaCl, and 10 mM imidazole. Cells were lysed by a French press (Constant Systems Ltd, Daventry, England). After centrifugation, the soluble protein in the supernatant was purified by Immobilized metal-assisted chromatography (IMAC). The purified fractions containing CP were pooled and dialyzed in 1X phosphate buffer saline (1X PBS) (1.8 mM KH_2PO_4,, 2.7 mM KCl, 10 mM Na_2HPO_4, and 137 mM NaCl, pH 7.4) at 4 °C for overnight and analyzed using 12% sodium dodecyl sulfate (SDS)-polyacrylamide gel electrophoresis (PAGE). Following dialysis, the protein was further utilized for the biophysical assay.

Binding kinetics analysis using Surface plasmon resonance (SPR)

The binding kinetics and affinity of identified compounds to the purified CP were investigated using SPR by a Biacore T200 system. The Ni-reagent kit (28995043, GE healthcare) method was used to immobilize CP over the Ni-NTA sensor chip (BR100532, GE healthcare). To prepare the Ni-NTA sensor chip, degassed and filtered 1X PBS running buffer was used for pre-conditioning prior to immobilization of his-tagged CP. The purified his-tagged CP was diluted to 5 µg/mL concentration in 1X PBS degassed and filtered buffer for immobilization on Ni-NTA sensor chips. Similarly, the compounds were diluted in degassed and filtered 1X PBS buffer and subsequently flown over the surface of immobilized his-tagged CP at a 30 µL/min flow rate. The contact time for compound-protein interaction was set to 60 s, followed by a dissociation time of 60 s. The surface was regenerated after each dissociation phase using 350 mM ethylenediamine tetraacetic acid (EDTA) (HiMedia). The SPR data were acquired and subsequently analyzed using the Biacore evaluation software. The equilibrium dissociation constants (K_D) for each interaction between the CP and the compound were calculated by fitting the data to a 1:1 Langmuir binding model.

Virus, cells, and compounds

The CHIKV patient sample isolate (Accession no. KY057363.1) (Singh et al., 2018) used in this study was propagated in Vero cells (NCCS, Pune, India). Vero cells were cultured in Dulbecco's modified eagle's medium (DMEM) (HiMedia) augmented with penicillin (100 U/mL) and streptomycin (100 µg/mL) (HiMedia) and 10% heat-inactivated Fetal bovine serum (FBS) (Gibco) at 37°C in the presence of 5% CO_2.

Efavirenz (E0997) and Dehydrocholic acid (D0042) were purchased from TCI Chemicals. Tomatidine (T2909) was purchased from Sigma and jervine (11723) was procured from Cayman. The stock solutions of efavirenz, dehydrocholic acid, and tomatidine were

prepared in dimethyl sulfoxide (DMSO) (HiMedia), while jervine was dissolved in ethanol (Merck). Working dilutions of the compounds for treating the cells were prepared by diluting the stock solutions in DMEM supplemented with 2% FBS.

Cell viability assay

The viability of the Vero cells in the presence of different compound concentrations was evaluated using 3-(4,5-dimethylthiazol-2-yl)-2,5-diphenyl tetrazolium bromide (MTT) (HiMedia) assay, as described previously (Fatma et al., 2020). Briefly, a 96-well plate containing Vero cells monolayer was incubated with 2-fold dilutions of compounds in DMEM containing 2% FBS for 24 h at 37°C and 5% CO_2. After 24 h of compound treatment, 20 µL of MTT (5mg/mL) was added per well. The cells were further incubated at 37°C in 5% CO_2 for 4 h. Upon incubation, formazan crystals were dissolved in DMSO and the absorbance was recorded at 570 nm using the plate reader (Thermo Fisher Scientific). The cell viability of the compound-treated cells was compared to that of the control (only solvent-treated). The 50% cytotoxic concentration (CC_{50}) values were calculated using GraphPad's non-linear regression curve fit analysis.

***In vitro* antiviral assay**

To evaluate the antiviral activity of compounds, a 24-well plate was seeded with Vero cells. The monolayer was infected by CHIKV or SINV with a multiplicity of infection (MOI) of 0.1 while gentle shaking every 15 min for 90 min, then washed with 1X PBS, and post-treatment with compounds was given for 24 h. Upon incubation, the media was harvested and subjected to a plaque assay to quantify the number of virus particles released in the supernatant. The 50% effective concentration (EC_{50}) value was calculated based on PFU/mL values obtained from the plaque assay.

Immunofluorescence assay

A confluent monolayer of Vero cells was infected by CHIKV or SINV (MOI 1) for 90 mins; subsequently, the monolayer was washed, and cells were incubated with 2-fold dilutions of compounds for 30 h. After incubation, cells were fixed with 1:1 ratio of methanol: acetone for 30 min. After 1X PBS wash, the cells were permeabilized by 0.1% Triton X-100 (Qualigens). Followed by 1X PBS wash, the anti-alphavirus mouse monoclonal antibody (Santa Cruz Biotechnology) was incubated with cells for 90 min. Wash was given to remove excess amounts of primary antibody, and secondary fluorescein isothiocyanate (FITC)-conjugated anti-mouse secondary antibody (Sigma) was added. Finally, cells were counterstained using 4',6-diamidino-2-phenylindole (DAPI) (HiMedia) and then observed under the EVOS FL imaging system (Thermo Fisher Scientific) using both DAPI and GFP channels. EVOS FL software was used to process the acquired images.

Intracellular CHIKV RNA assessment by quantitative reverse transcription polymerase chain reaction (qRT-PCR)

Total RNA was isolated from the cells by using Takara RNAiso Plus as per the manufacturer's instructions. Isolated RNA was quantified with the help of nanodrop, and a further 1µg RNA was used to synthesize cDNA by the PrimeScript first-strand cDNA synthesis kit (Takara Bio, Kusatsu, Japan). E1 gene-specific primers were used as previously described (Singh et al., 2018), and β-actin was kept as an internal control, using the KAPA SYBR fast universal qPCR kit on the QuantStudioTM 5 system (Applied Biosystems, Waltham, MA, USA). The qRT-PCR reactions were performed in duplicate, and the ΔΔCt method was used for calculating the relative quantification (RQ) value ($RQ = 2^{-\Delta\Delta Ct}$).

Time of compound addition experiment

Vero cells were treated with 6.25 µM and 3.25 µM concentrations of efavirenz at pre-infection, at the time of infection (ATI) or post-infection. For pre-treatment, efavirenz was added 2 h before the infection (CHIKV MOI 0.1) and then the cells were washed with PBS twice. For ATI condition, efavirenz was added in the virus inoculum and cells were infected for 2 h. In the case of post-treatment, cells were treated with efavirenz at 0, 2, 4, 6, 8, 10, 12 h after infection. For all time point condition, virus infection was done for 2 hours and the supernatant was harvested after 24 hours of virus infection. Percentage virus inhibition was quantified using plaque assay as described previously.

Results

Computational-assisted screening and pharmacokinetics analysis

The compounds that showed Binding energy (B.E.) of more than 8 kcal/mol and greater than the cdE2 peptide (Thr 398 - Val 408) were shortlisted (Supplementary Table 1). The cdE2 peptide with the sequence Thr-Pro-Tyr-Glu-Leu-Thr-Pro-Gly-Ala-Thr-Val (Thr398- Val408) revealed a B.E. of -6.7 kcal/moL when docked against the hydrophobic pocket of CP. The docking result suggests that the binding affinity of the peptide is lower than the selected screened compounds, as shown in figure 1 and Table 1. Based on virtual screening, the compounds showing B.E >8 kcal/mol were selected and subjected to a drug-likeness study using the SWISS-ADME analysis tool. Utilizing the bioavailability radar analysis, the list was further narrowed down to four promising drug candidates from the screened 51 compounds (Supplementary Table 2), employing the Swiss ADME online analysis tool. Notably, the compounds jervine, efavirenz, dehydrocholic acid and tomatidine from the library met the Lipinski rule criteria, suggesting their potential suitability as drug candidates (M. Q. Zhang & Wilkinson, 2007). The detailed physicochemical properties of the four shortlisted compounds

are shown in Supplementary Figure 1 and Supplementary Table 2, providing comprehensive information for further evaluation and analysis.

.

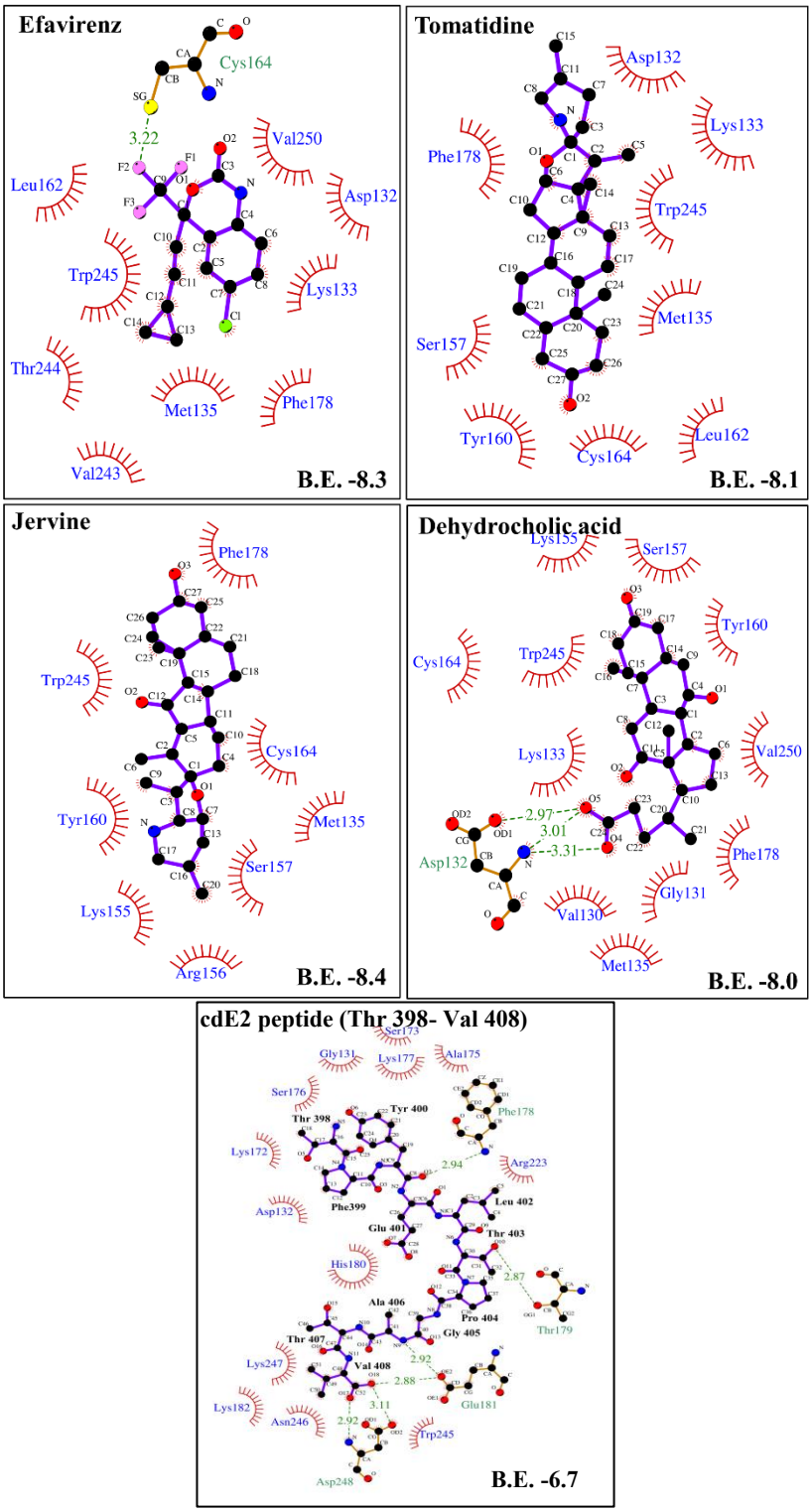

Figure 1: *Schematic representation of selected compounds and cdE2 peptide showcasing their interactions with the hydrophobic pocket of CP using the LIGPLOT+ analysis tool. This representation highlights both hydrophobic (Brown color curvature) and H-bond interactions (Green dashed line), and the binding energy associated with these interactions.*

Table 1: *The chemical structure of compounds with their hydrophobic and H-bond interactions against hydrophoboc pocket of CP.*

Compounds	Structure	Binding Energy (kcal/mol)	H-bond				Hydrophobic Interactions
			Residue No.	No. of Bonds	Molecules	Bond Length (A^0)	
Peptide	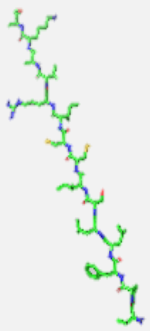	-6.7	Phe178	1	N-O2	2.94	Gly131, Asp132, Lys172, Ser173, Ala175, Ser176, Lys177, His180, Lys182, Arg223, Trp245, Asn246, Lys247
			Thr179	1	OG1-O10	2.87	
			Asp248	2	N-O17	2.92	
					OD2-O18	3.11	
			Glu181	2	OE2-O18	2.88	
					OE2-N9	2.92	
Efavirenz	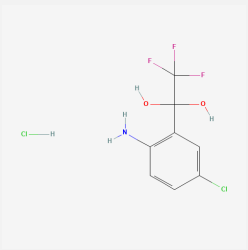	-8.3	Cys164	1	SG-F2	3.22	Asp132, Lys133, Met135, Leu162, Phe178, Val243, Thr244, Trp245, Val250
Tomatidine	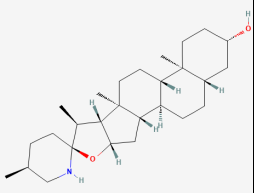	-8.1	-	-	-	-	Asp132, Lys133, Met135, Ser157, Tyr160, Leu162, Cys164, Phe178, Trp245
Jervine	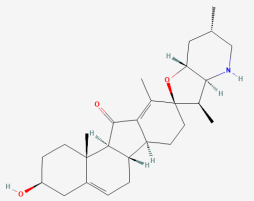	-8.4	-	-	-	-	Met135, Lys155, Arg156, Ser157, Tyr160, Cys164, Phe178, Trp245
Dehydrocholic acid		-8.0	Asp132	3	OD1-O5	2.97	Val130,

	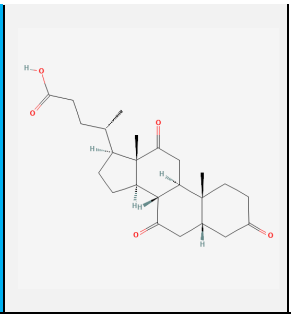				N-O5	3.01	Gly131, Lys133, Met135, Lys155, Ser157, Tyr160, Cys164, Phe178, Trp245 Val250
					N-O4	3.31	

The four selected compounds were also subjected to molecular re-docking study for detailed analysis of binding interactions with the CP. All the selected compounds exhibited hydrophobic interactions with the targeted amino acids in the hydrophobic pocket of the CP. The compounds also displayed B.E. ranging from -8.0 to -8.3 kcal/mol (Table 1), while efavirenz and jervine displayed the maximum B.E. The compounds' binding affinity and their bonding interactions with CP are summarized in Figure 1 and Table 1.

Characterization of compound binding to the capsid protein

The combination of screening and pharmacokinetic studies enabled the selection of four compounds for further characterization of their binding affinities with the purified CP (Supplementary figure 2). We investigated the affinity of efavirenz and dehydrocholic acid towards CP in the range of 1 to 200 µM. Tomatidine and jervine precipitated at concentrations higher than 25 µM, thus binding with the CP cannot be determined beyond a concentration of 25 µM. Increasing efavirenz concentration from 12.5 µM to 200 µM was injected over the CP-immobilized sensor surface revealed that the efavirenz–CP interactions were strongly dosage-dependent and obtained equilibrium dissociation constant (K_D) of 6.22 µM (Figure 2). Evaluation of the efavirenz binding efficiency emphasized the importance of residence time, and thus, the 1:1 Langmuir kinetic fitting model was examined to determine the association rate constant (k_{on}), as 770 $M^{-1}s^{-1}$, and the dissociation rate constant (k_{off}) as 0.004799 s^{-1}.

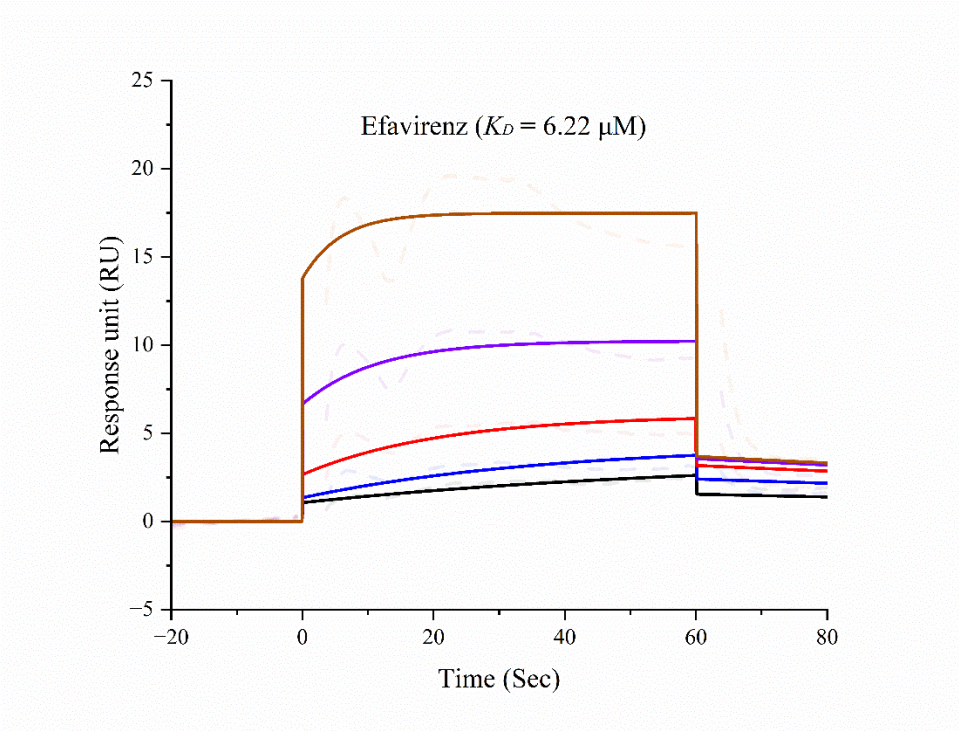

Figure 2: *SPR sensorgram elucidating binding kinetics analysis of efavirenz onto the immobilized CP. The different colour-coded lines represent the varying efavirenz concentration (12.5 – 200 µM) injected onto the sensor surface of immobilized CP to detect the kinetic affinity.*

Evaluation of cell viability and broad-spectrum anti-alphavirus activity of compounds

Prior to evaluating anti-alphavirus activity of compounds, cytotoxicity was determined by MTT assay. The CC_{50} values were 53.62 and 17.19 µM for efavirenz and tomatidine, respectively. Anti-CHIKV and anti-SINV activity were determined by quantitative evaluation of progeny virus particles released in the supernatant of cells in the presence of 2-fold dilutions of compounds below cytotoxic concentration. Efavirenz (EC_{50} = 1.33 µM) and tomatidine (EC_{50} = 5.35 µM) showed dose-dependent inhibition of CHIKV propagation, which was observed well below cytotoxic concentration (Figure 3A and 3B). Similarly, efavirenz and Tomatidine inhibited the SINV replication at the EC_{50} values of 0.7 µM and 2.47 µM (Figure

3C and 3D). Dehydrocholic acid failed to inhibit the replication of both the alphaviruses below their cytotoxic concentration. The antiviral properties of jervine cannot be determined due to the insolubility of jervine in an aqueous solution at desired concentrations.

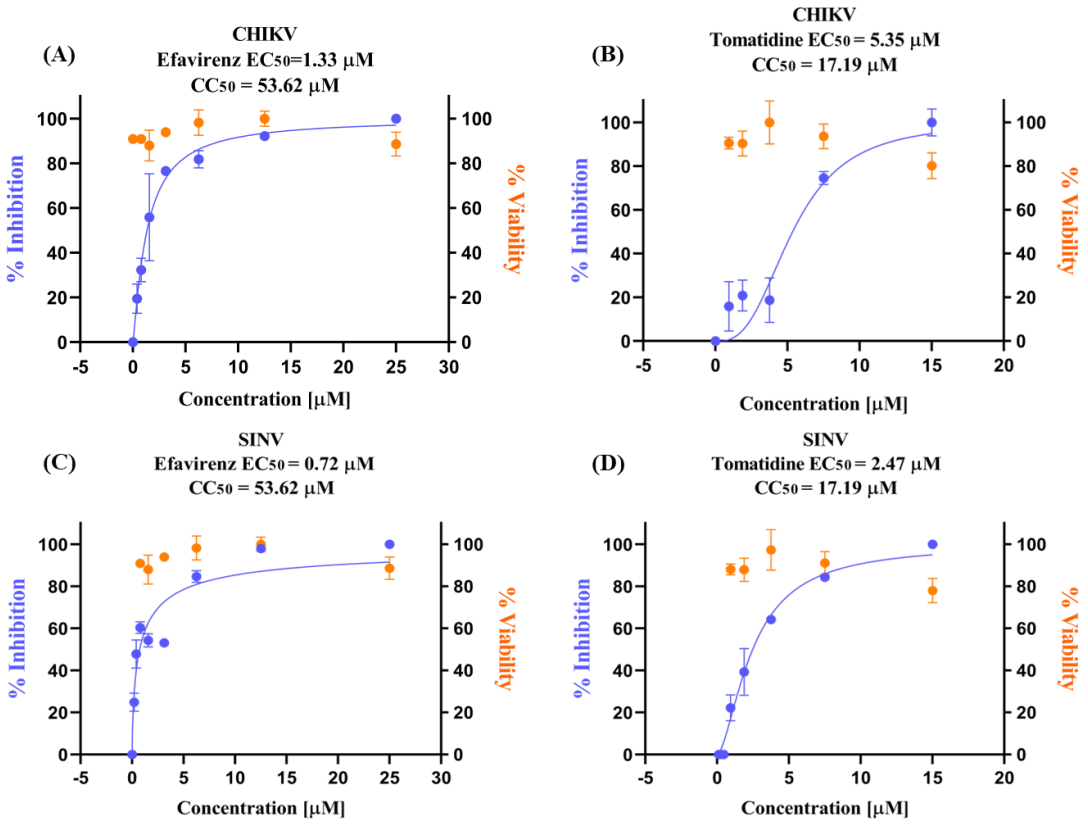

Figure 3: *Comparitive in-vitro inhibitory effect of Efavirenz and Tomatidine against CHIKV (A and B) and SINV (C and D). The decrease in virus titre in the presence of an increasing compound concentration was assessed by plaque assay. The CHIKV and SINV titre in the supernatant was evaluated 24 hours post-infection. The percentage inhibition was calculated by considering 100% viral titre in corresponding vehicle-treated cells. The 50 % effective concentration (EC_{50}) value was determined by GraphPad prism by using non-linear fit model after data normalization. The values are the mean of two independent experiments and the error bar shows the standard deviation. The orange and blue data points represent cell viability and percentage virus inhibition, respectively.*

The intracellular replication inhibition of CHIKV and SINV was studied by IFA with the help of primary anti-alphavirus mouse monoclonal antibody and secondary FITC-conjugated antibodies. Concentration-dependent reduction in intracellular fluorescence was observed for efavirenz and tomatidine-treated cells (Figure 4). Further, the reduction in the abundance of intracellular CHIKV RNA due to efavirenz treatment was detected by qRT-PCR. Significant fold change in the intracellular CHIKV RNA was observed (Figure 5). Thus, collectively plaque-based antiviral assay, IFA, and qRT-PCR prove the excellent anti-CHIKV activity of efavirenz.

A) CHIKV inhibition

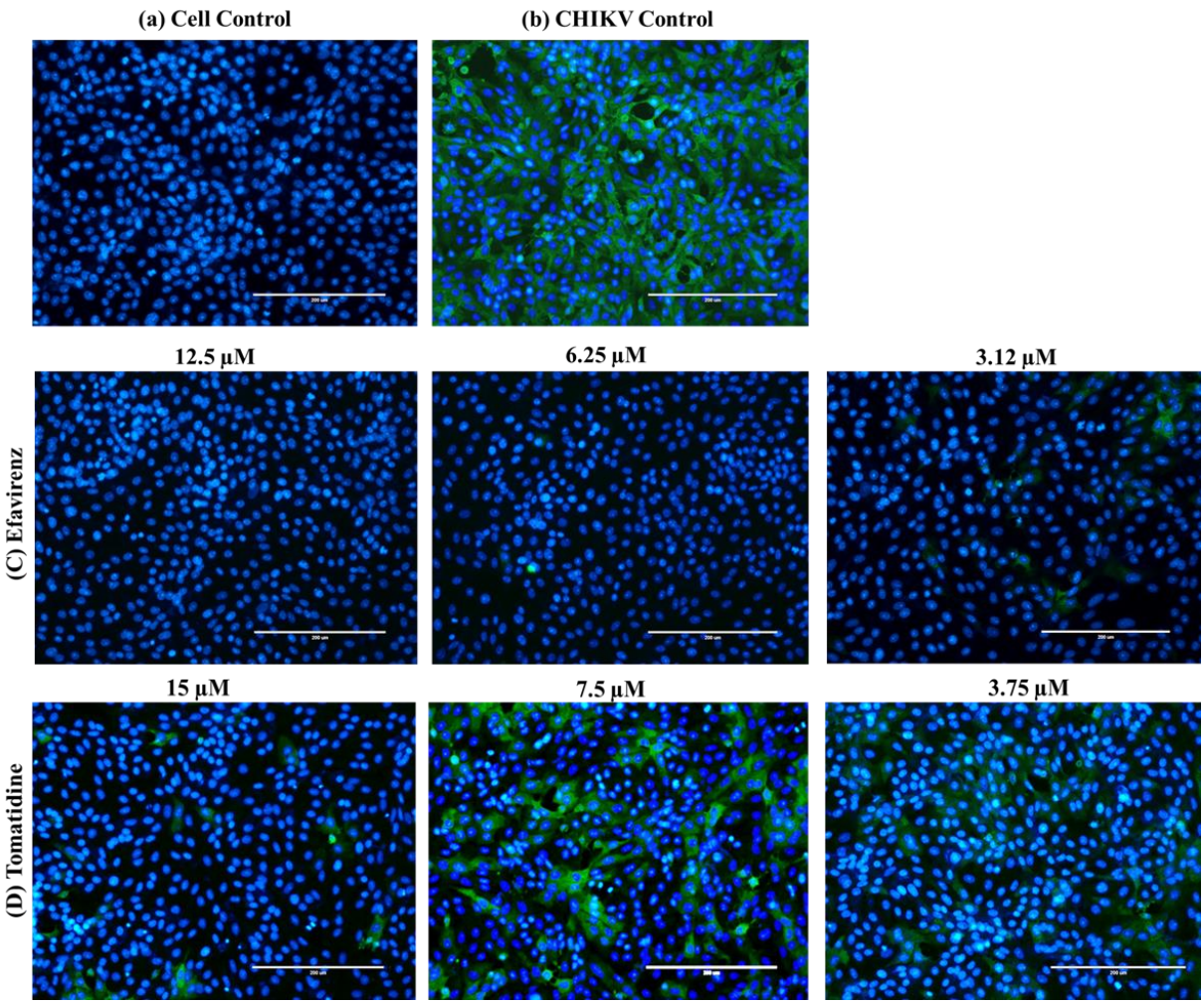

B) SINV inhibition

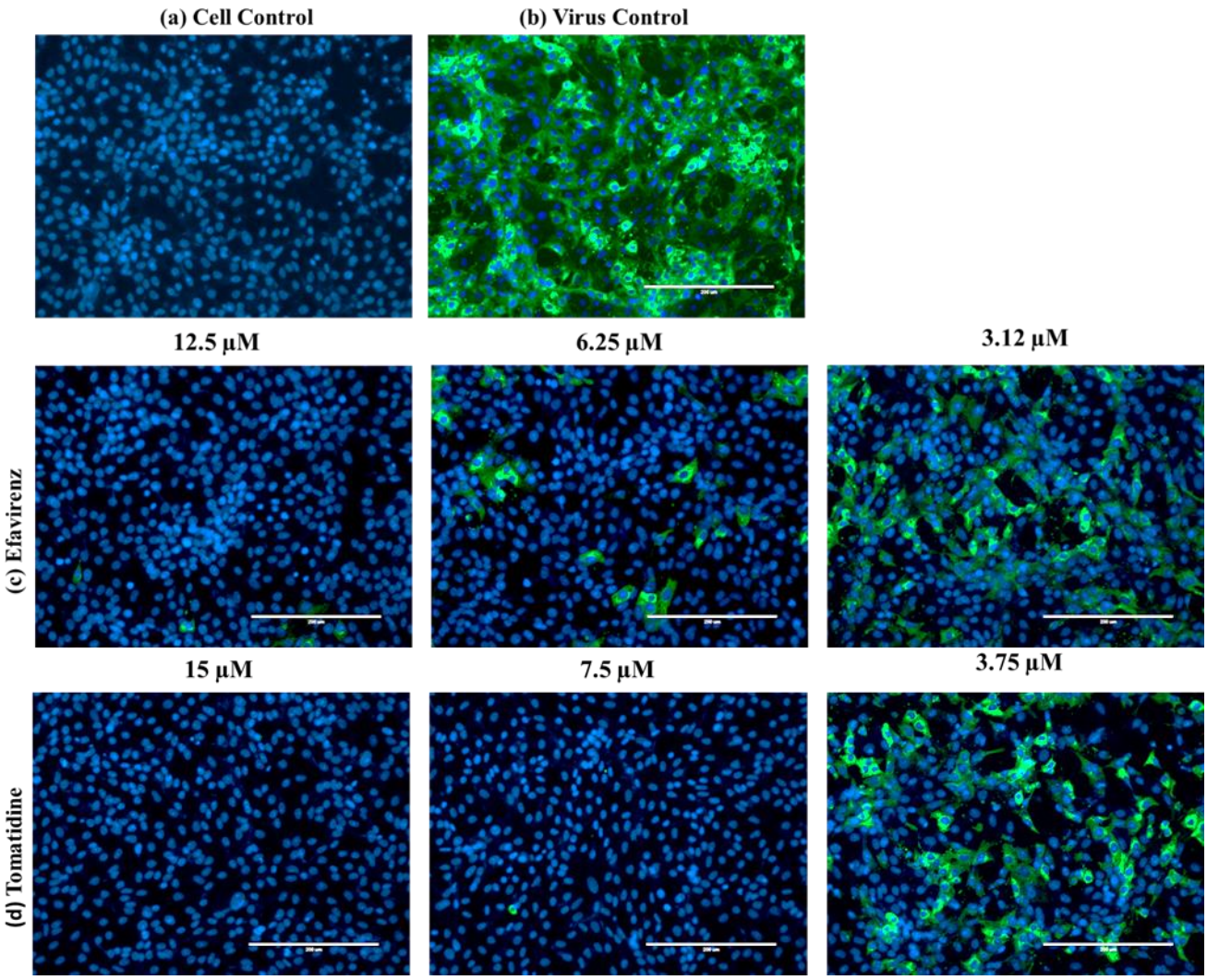

Figure 4: *Detection of A) CHIKV and B) SINV inhibition by efavirenz and tomatidine with the help of immunofluorescence microscopy. The cells were infected and then treated with different concentrations of compounds, as shown in the figure. After 30 hours post-infection, the cells were fixed and the presence of replicated intracellular virus was detected by anti-alphavirus antibodies and fluorescein isothiocyanate (FITC)-conjugated secondary antibody. The images were captured at 20 X magnification. Scale bar, 200 µM.*

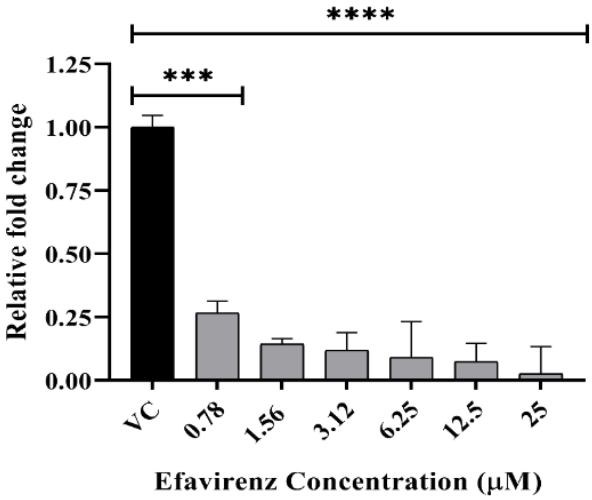

Figure 5: *Relative fold change in the intracellular viral RNA due to efavirenz treatment as compared to virus control (VC) was assessed by qRT-PCR. Total RNA was isolated 24 hpi and expression of E1 gene was quantified using E1 specific primers. The data was analyzed by the one-way ANOVA test and Dunnett's posttest; ****, P < 0.0001. ***, P = 0.0002. The error bar shows the standard deviation of the duplicate set of reactions (n = 2).*

Evaluation of inhibition step of CHIKV life cycle by efavirenz

A time-of-addition experiment was performed further to understand the kinetics of the antiviral activity of efavirenz. Vero cells were treated with two different concentrations of efavirenz (6.25 µM and 3.12 µM) during different time periods, such as 2 h before infection (Pre), at the ATI or simultaneous and post 0, 2, 4, 6, 8, 10 and 12 h time points after infection (Figure 6). At both the tested concentrations, efavirenz most potently inhibited the replication of CHIKV up to 8 h of post-treatment.

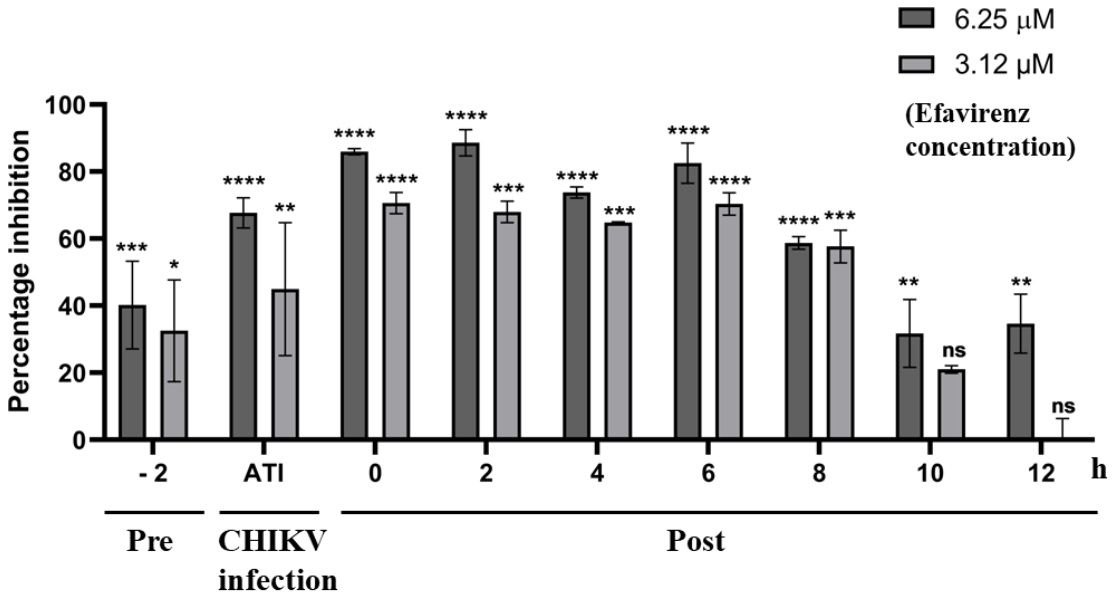

Figure 6*: The most potent inhibitory effect of efavirenz is observed in the post-treatment of the compound up to 8 h of infection. Vero cells were infected with CHIKV (MOI = 0.1), and cells were treated before infection (-2 h), during infection and post-infection (0 to 12 h) at indicated time points. The data was analyzed by the one-way ANOVA test and Dunnett's test; ****, P < 0.0001. ***, P = 0.0001. **, P = 0.0023. *, P = 0.0198. ns, non-significant. The error bar shows the mean values' standard deviation (n = 2).*

Discussion

CHIKV is a recurring alphavirus with a global presence in tropical and sub-tropical regions that lacks effective antiviral drugs or vaccines. A promising approach to combat this virus involves disrupting the crucial interaction between cdE2 and the hydrophobic pocket of CP, which plays a pivotal role in CHIKV budding. In our current study, we employed structure-based virtual screening to identify potential molecules capable of binding to the hydrophobic pocket of CP, based on their obtained binding energies. Subsequently, four compounds, namely jervine, efavirenz, dehydrocholic acid and tomatidine, were shortlisted according to favorable physiochemical properties, including solubility, size, lipophilicity, H-bond acceptor, and donor

characteristics. These selected compounds also fulfilled the criteria of Lipinski rule. Among these shortlisted compounds, jervine and tomatidine are natural steroidal alkaloids derived from *Veratrum californicum* (Bailly et al., 2016) and unripe green tomatoes (Troost et al., 2020), respectively. Dehydrocholic acid, on the other hand, is a synthetic bile acid (Soloway et al., 1973), and efavirenz is a non-nucleoside inhibitor of HIV reverse transcriptase, used for treating HIV type 1 infection and or to prevent the spread of HIV (Costa & Vale, 2023). To evaluate their binding affinity to the CP, we employed the highly sensitive SPR technique and successfully determined the binding of efavirenz and dehydrocholic acid to CP within a concentration range of 1 to 200 μM. Notably, efavirenz showed a good binding affinity towards capsid with the K_D value of 6.22 μM (Figure 2). The binding of dehydrocholic acid with CP was not observed. The binding of tomatidine and jervine at a concentration exceeding 25 μM cannot be determined due to insolubility issues in aqueous solution at higher concentrations, limiting our ability to evaluate affinity towards the CP. These results suggest that efavirenz may potentially target the CP within the host cell by binding to hydrophobic pocket, inhibiting virus replication at the late stage.

To further validate this assumption, cell culture-based studies were conducted to investigate the potency of efavirenz against CHIKV and also against SINV to check broad anti-alphavirus activity as the hydrophobic pocket is conserved in alphaviruses (Sharma et al., 2016). Virus-infected cells were incubated with gradually decreasing concentrations of the compounds for 24 hpi, and subsequent extracellular infectious virus particle titre was evaluated via plaque assay, while intracellular viral replication was detected by IFA. In the case of CHIKV, the abundance of intracellular RNA was assessed by qRT-PCR. The EC_{50} values were calculated based on the results obtained from the plaque assay, the efavirenz exhibited highly effective inhibition of CHIKV replication, with a low micromolar EC_{50} value of 1.33 μM (Figure 3A) and also inhibited SINV replication (EC_{50}= 0.7 μM) (Figure 3C). Additionally, a

significant decrease in CHIKV intracellular RNA was observed as compared to virus control (VC) in qRT-PCR (Figure 5). To further gain a better understanding of step of CHIKV inhibition by efavirenz, time of compound addition experiment was performed. Most significant inhibition of CHIKV was observed in the post-treatment up to 8 hours of infection (Figure 6). The CHIKV budding step is the last step in the life cycle of virus. Thus, the time of compound addition study indicates that replication might be inhibited during the late stage of virus infection, such as virus budding. IFA was employed to evaluate intracellular alphavirus replication in both compounds treated and non-treated cells after infection. A drastic reduction in the number of infected cells was observed upon compound treatment as compared to the virus control (Figure 4A and 4B). Notably, tomatidine among these four compounds has already been reported to exhibit anti-CHIKV activity, so it acted as a positive control for antiviral assays, and there is speculation that it might target the CP of CHIKV (Troost et al., 2020). Encouragingly, our *in-silico* study also revealed that tomatidine has favourable binding energy towards the hydrophobic pocket of CP. As a result, tomatidine was selected for further evaluation, aiming to determine its binding to the hydrophobic pocket in more detail. However, due to low solubility above 25 μM concentration, the affinity of tomatidine towards the CP cannot be evaluated with the help of SPR. Berit Troost et. al reported EC_{50} values of tomatidine against different strains of CHIKV in the range of 1.3 to 3.8 μM. As compared to Berit Troost et. al. in our experimental settings, we obtained the EC_{50} value of 5.35 μM for tomatidine. In addition to this, anti-SINV activity of tomatidine was unknown. Here, we proved that tomatidine inhibits SINV propagation also (EC_{50}= 2.47 μM). It is noteworthy that tomatidine's inhibitory effect extends beyond CHIKV, as it has also demonstrated activity against Zika and Dengue viruses (Diosa-Toro et al., 2019).

Previously, Varghase et. al. evaluated anti-CHIKV activity of efavirenz by CHIKV replicons which lacks the structural protein; they did not observe significant inhibition in the

replicon assay; thus, they did not proceed further to test anti-CHIKV activity on the wild type virus (Varghese et al., 2016). The logical reason for the little inhibitory effect against CHIKV replicon of efavirenz is that the replicon lacks the structural protein, and as proposed in the present study, the efavirenz is acting on CP, one of the structural proteins. Efavirenz is a well-known inhibitor of HIV reverse transcriptase, it is the first-generation non-nucleoside reverse transcriptase inhibitor (NNRTI) used to treat acquired immunodeficiency syndrome (AIDS). Efavirenz inhibits the activity of HIV RNA-directed DNA polymerase (reverse transcriptase) by binding to the hydrophobic region of HIV-1 reverse transcriptase (RT) (Maggiolo, 2007). The LIGPLOT+ analysis of the crystal structure of HIV reverse transcriptase in complex with efavirenz (*Supplementary figure 3)* and efavirenz interaction with hydrophobic pocket of CP (Figure 1) indicates some common residues involved in hydrophobic interaction with efavirenz. LIGPLOT+ analysis showed both the hydrophobic regions of HIV reverse transcriptase and CHIKV CP have the following common residues Valine, Lysine, Phenylalanine, Tryptophane and Leucine which are involved in hydrophobic interaction with efavirenz. Efavirenz is extensively used in the antiretroviral regimen to treat HIV-infected patients in developing countries because of its efficacy, affordability, low cost, and convenience (Nachega et al., 2008). Efavirenz also has antiviral activity against Zika and West Nile Virus (Sariyer et al., 2019; Stefanik et al., 2020). The oral bioavailability of efavirenz is good and it also has a long half-life. When a single oral dose of 100 to 1600 mg is administered to healthy volunteers, the peak efavirenz plasma concentrations of 1.6 – 9.1 μM reach after 5 hours of dose. On average it takes 3 – 5 h to reach peak plasma concentrations and steady-state plasma concentrations are reached in 6 – 10 days (Vrouenraets et al., 2007).

In conclusion, we predicted efavirenz with another three compounds tomatidine, jervine and dehydrocholic acid, as potential compounds that can interact with the hydrophobic pocket of CP with the help of *in silico* tools. Further, the binding of efavirenz with CP was validated

by SPR. The possible anti-CHIKV and anti-SINV activity of efavirenz, which might occur due to binding with the hydrophobic pocket of CP resulting into disruption of cdE2 interaction with CP was evaluated by *in vitro* antiviral assays. Cell culture-based antiviral assay, Immunofluorescence assay and qRT-PCR have proved excellent anti-CHIKV activity of efavirenz. All together *in silico*, biophysical and cell culture-based antiviral assay and known good oral bioavailability of efavirenz, we propose that efavirenz can act as an effective antiviral drug to treat the CHIKV infection.

Acknowledgement:

This research was funded by ICMR Ref no. ISRM/12(46)/2020. S.N. thank the Ministry of Human Resource Development (MHRD), and R.R thank the University Grants Commission (UGC), Government of India, for a research fellowship. The authors also thank the Department of Biosciences and Bioengineering (BSBE), Government of India, for supporting Bioinformatics Centre at IIT Roorkee (reference number BT/PR40141/BTIS/137/16/2021). The authors acknowledge and thank the Macromolecular Crystallographic Facility (MCU) and Bioinformatics centre at IIC, Indian Institute of Technology, Roorkee.

References

1. Abdelnabi, R., Neyts, J., & Delang, L. (2015). Towards antivirals against chikungunya virus. In *Antiviral Research* (Vol. 121). https://doi.org/10.1016/j.antiviral.2015.06.017
2. Aggarwal, M., Kaur, R., Saha, A., Mudgal, R., Yadav, R., Dash, P. K., Parida, M., Kumar, P., & Tomar, S. (2017). Evaluation of antiviral activity of piperazine against Chikungunya virus targeting hydrophobic pocket of alphavirus capsid protein. *Antiviral Research*, *146*, 102–111. https://doi.org/10.1016/j.antiviral.2017.08.015
3. Bailly, B., Richard, C. A., Sharma, G., Wang, L., Johansen, L., Cao, J., Pendharkar, V., Sharma, D. C., Galloux, M., Wang, Y., Cui, R., Zou, G., Guillon, P., Von Itzstein, M., Eléouët, J. F., & Altmeyer, R. (2016). Targeting human respiratory syncytial virus transcription anti-termination factor M2-1 to inhibit in vivo viral replication. *Scientific Reports*, *6*. https://doi.org/10.1038/srep25806
4. Bodenmann, P., & Genton, B. (2006). Chikungunya: an epidemic in real time. *Lancet*, *368*(9531). https://doi.org/10.1016/S0140-6736(06)69046-6
5. Brown, T. (2014). ChemDraw. *The Science Teacher*, *81*(2).
6. Cassadou, S., Boucau, S., Petit-Sinturel, M., Huc, P., Leparc-Goffart, I., & Ledrans, M. (2014). Emergence of chikungunya fever on the French side of Saint Martin island, October to December 2013. *Eurosurveillance*, *19*(13). https://doi.org/10.2807/1560-7917.ES2014.19.13.20752
7. Chretien, J. P., Anyamba, A., Bedno, S. A., Breiman, R. F., Sang, R., Sergon, K., Powers, A. M., Onyango, C. O., Small, J., Tucker, C. J., & Linthicum, K. J. (2007). Drought-associated chikungunya emergence along coastal East Africa. *American Journal of Tropical Medicine and Hygiene*, *76*(3). https://doi.org/10.4269/ajtmh.2007.76.405
8. Costa, B., & Vale, N. (2023). Efavirenz: History, Development and Future. In

Biomolecules (Vol. 13, Issue 1). https://doi.org/10.3390/biom13010088

9. Daina, A., Michielin, O., & Zoete, V. (2017). SwissADME: A free web tool to evaluate pharmacokinetics, drug-likeness and medicinal chemistry friendliness of small molecules. *Scientific Reports*, *7*. https://doi.org/10.1038/srep42717
10. Daina, A., & Zoete, V. (2016). A BOILED-Egg To Predict Gastrointestinal Absorption and Brain Penetration of Small Molecules. *ChemMedChem*. https://doi.org/10.1002/cmdc.201600182
11. Diosa-Toro, M., Troost, B., van de Pol, D., Heberle, A. M., Urcuqui-Inchima, S., Thedieck, K., & Smit, J. M. (2019). Tomatidine, a novel antiviral compound towards dengue virus. *Antiviral Research*, *161*. https://doi.org/10.1016/j.antiviral.2018.11.011
12. Erin Staples, J., Breiman, R. F., & Powers, A. M. (2009). Chikungunya fever: An epidemiological review of a re-emerging infectious disease. In *Clinical Infectious Diseases* (Vol. 49, Issue 6). https://doi.org/10.1086/605496
13. Fatma, B., Kumar, R., Singh, V. A., Nehul, S., Sharma, R., Kesari, P., Kuhn, R. J., & Tomar, S. (2020). Alphavirus capsid protease inhibitors as potential antiviral agents for Chikungunya infection. *Antiviral Research*, *179*. https://doi.org/10.1016/j.antiviral.2020.104808
14. Holland Cheng, R., Kuhn, R. J., Olson, N. H., Rossmann Hok-Kin Choi, M. G., Smith, T. J., & Baker, T. S. (1995). Nucleocapsid and glycoprotein organization in an enveloped virus. *Cell*, *80*(4). https://doi.org/10.1016/0092-8674(95)90516-2
15. Jose, J., Przybyla, L., Edwards, T. J., Perera, R., Burgner, J. W., & Kuhn, R. J. (2012). Interactions of the Cytoplasmic Domain of Sindbis Virus E2 with Nucleocapsid Cores Promote Alphavirus Budding. *Journal of Virology*, *86*(5). https://doi.org/10.1128/jvi.05860-11
16. Khan, A. H., Morita, K., del Carmen Parquet, M., Hasebe, F., Mathenge, E. G. M., &

Igarashi, A. (2002). Complete nucleotide sequence of chikungunya virus and evidence for an internal polyadenylation site. *Journal of General Virology*, *83*(12). https://doi.org/10.1099/0022-1317-83-12-3075

17. Kim, H. Y., Kuhn, R. J., Patkar, C., Warrier, R., & Cushman, M. (2007). Synthesis of dioxane-based antiviral agents and evaluation of their biological activities as inhibitors of Sindbis virus replication. *Bioorganic and Medicinal Chemistry*, *15*(7). https://doi.org/10.1016/j.bmc.2007.01.040
18. Kim, H. Y., Patkar, C., Warrier, R., Kuhn, R., & Cushman, M. (2005). Design, synthesis, and evaluation of dioxane-based antiviral agents targeted against the Sindbis virus capsid protein. *Bioorganic and Medicinal Chemistry Letters*, *15*(13). https://doi.org/10.1016/j.bmcl.2005.05.013
19. Kostyuchenko, V. A., Jakana, J., Liu, X., Haddow, A. D., Aung, M., Weaver, S. C., Chiu, W., & Lok, S.-M. (2011). The Structure of Barmah Forest Virus as Revealed by Cryo-Electron Microscopy at a 6-Angstrom Resolution Has Detailed Transmembrane Protein Architecture and Interactions. *Journal of Virology*, *85*(18). https://doi.org/10.1128/jvi.05015-11
20. Kovacikova, K., & van Hemert, M. J. (2020). Small-Molecule Inhibitors of Chikungunya Virus: Mechanisms of Action and Antiviral Drug Resistance. In *Antimicrobial Agents and Chemotherapy* (Vol. 64, Issue 12). https://doi.org/10.1128/AAC.01788-20
21. Lee, S., Kuhn, R. J., & Rossmann, M. G. (1998). Probing the potential glycoprotein binding site of Sindbis virus capsid protein with dioxane and model building. *Proteins: Structure, Function and Genetics*, *33*(2). https://doi.org/10.1002/(SICI)1097-0134(19981101)33:2<311::AID-PROT13>3.0.CO;2-N
22. Lee, S., Owen, K. E., Choi, H. K., Lee, H., Lu, G., Wengler, G., Brown, D. T.,

Rossmann, M. G., & Kuhn, R. J. (1996). Identification of a protein binding site on the surface of the alphavirus nucleocapsid and its implication in virus assembly. *Structure*, *4*(5). https://doi.org/10.1016/S0969-2126(96)00059-7

23. Maggiolo, F. (2007). Efavirenz. *Http://Dx.Doi.Org/10.1517/14656566.8.8.1137*, *8*(8), 1137–1145. https://doi.org/10.1517/14656566.8.8.1137
24. Mancini, E. J., Clarke, M., Gowen, B. E., Rutten, T., & Fuller, S. D. (2000). Cryo-electron microscopy reveals the functional organization of an enveloped virus, Semliki Forest virus. *Molecular Cell*, *5*(2). https://doi.org/10.1016/S1097-2765(00)80421-9
25. Melton, J. V., Ewart, G. D., Weir, R. C., Board, P. G., Lee, E., & Gage, P. W. (2002). Alphavirus 6K proteins form ion channels. *Journal of Biological Chemistry*, *277*(49). https://doi.org/10.1074/jbc.M207847200
26. Nachega, J. B., Hislop, M., Dowdy, D. W., Gallant, J. E., Chaisson, R. E., Regensberg, L., & Maartens, G. (2008). Efavirenz versus nevirapine-based initial treatment of HIV infection: clinical and virological outcomes in Southern African adults. *AIDS (London, England)*, *22*(16), 2117–2125. https://doi.org/10.1097/QAD.0B013E328310407E
27. Pialoux, G., Gaüzère, B. A., Jauréguiberry, S., & Strobel, M. (2007). Chikungunya, an epidemic arbovirosis. In *Lancet Infectious Diseases* (Vol. 7, Issue 5). https://doi.org/10.1016/S1473-3099(07)70107-X
28. Powers, A. M., & Logue, C. H. (2007). Changing patterns of chikunya virus: Re-emergence of a zoonotic arbovirus. In *Journal of General Virology* (Vol. 88, Issue 9). https://doi.org/10.1099/vir.0.82858-0
29. Puntasecca, C. J., King, C. H., & Labeaud, A. D. (2021). Measuring the global burden of Chikungunya and Zika viruses: A systematic review. In *PLoS Neglected Tropical Diseases* (Vol. 15, Issue 3). https://doi.org/10.1371/journal.pntd.0009055
30. Pushpakom, S., Iorio, F., Eyers, P. A., Escott, K. J., Hopper, S., Wells, A., Doig, A.,

Guilliams, T., Latimer, J., McNamee, C., Norris, A., Sanseau, P., Cavalla, D., & Pirmohamed, M. (2018). Drug repurposing: Progress, challenges and recommendations. In *Nature Reviews Drug Discovery* (Vol. 18, Issue 1). https://doi.org/10.1038/nrd.2018.168

31. Rani, R., Long, S., Pareek, A., Dhaka, P., Singh, A., Kumar, P., McInerney, G., & Tomar, S. (2022). Multi-target direct-acting SARS-CoV-2 antivirals against the nucleotide-binding pockets of virus-specific proteins. *Virology*, *577*, 1–15. https://doi.org/10.1016/J.VIROL.2022.08.008
32. Robinson, M. C. (1955). An epidemic of virus disease in southern province, tanganyika territory, in 1952–1953. i. clinical features. *Transactions of the Royal Society of Tropical Medicine and Hygiene*, *49*(1). https://doi.org/10.1016/0035-9203(55)90080-8
33. Ryan, S. J., Carlson, C. J., Mordecai, E. A., & Johnson, L. R. (2018). Global expansion and redistribution of Aedes-borne virus transmission risk with climate change. *PLoS Neglected Tropical Diseases*, *13*(3). https://doi.org/10.1371/journal.pntd.0007213
34. Sanz, M. A., Madan, V., Carrasco, L., & Nieva, J. L. (2003). Interfacial domains in sindbis virus 6K protein: Detection and functional characterization. *Journal of Biological Chemistry*, *278*(3). https://doi.org/10.1074/jbc.M206611200
35. Sariyer, I. K., Gordon, J., Burdo, T. H., Wollebo, H. S., Gianti, E., Donadoni, M., Bellizzi, A., Cicalese, S., Loomis, R., Robinson, J. A., Carnevale, V., Steiner, J., Ozdener, M. H., Miller, A. D., Amini, S., Klein, M. L., & Khalili, K. (2019). Suppression of Zika Virus Infection in the Brain by the Antiretroviral Drug Rilpivirine. *Molecular Therapy*, *27*(12). https://doi.org/10.1016/j.ymthe.2019.10.006
36. Sharma, R., Fatma, B., Saha, A., Bajpai, S., Sistla, S., Dash, P. K., Parida, M., Kumar, P., & Tomar, S. (2016). Inhibition of chikungunya virus by picolinate that targets viral capsid protein. *Virology*, *498*, 265–276. https://doi.org/10.1016/J.VIROL.2016.08.029

37. Sharma, R., Kesari, P., Kumar, P., & Tomar, S. (2018). Structure-function insights into chikungunya virus capsid protein: Small molecules targeting capsid hydrophobic pocket. *Virology*, *515*, 223–234. https://doi.org/10.1016/j.virol.2017.12.020
38. Singh, H., Mudgal, R., Narwal, M., Kaur, R., Singh, V. A., Malik, A., Chaudhary, M., & Tomar, S. (2018). Chikungunya virus inhibition by peptidomimetic inhibitors targeting virus-specific cysteine protease. *Biochimie*, *149*, 51–61. https://doi.org/10.1016/J.BIOCHI.2018.04.004
39. Solignat, M., Gay, B., Higgs, S., Briant, L., & Devaux, C. (2009). Replication cycle of chikungunya: A re-emerging arbovirus. In *Virology* (Vol. 393, Issue 2). https://doi.org/10.1016/j.virol.2009.07.024
40. Soloway, R. D., Hofmann, A. F., Thomas, P. J., Schoenfield, L. J., & Klein, P. D. (1973). Triketocholanoic (dehydrocholic) acid. Hepatic metabolism and effect on bile flow and biliary lipid secretion in man. *The Journal of Clinical Investigation*, *52*(3). https://doi.org/10.1172/JCI107233
41. Stefanik, M., Valdes, J. J., Ezebuo, F. C., Haviernik, J., Uzochukwu, I. C., Fojtikova, M., Salat, J., Eyer, L., & Ruzek, D. (2020). Fda-approved drugs efavirenz, tipranavir, and dasabuvir inhibit replication of multiple flaviviruses in vero cells. *Microorganisms*, *8*(4). https://doi.org/10.3390/microorganisms8040599
42. Strauss, J. H., & Strauss, E. G. (1994). The alphaviruses: Gene expression, replication, and evolution. In *Microbiological Reviews* (Vol. 58, Issue 3). https://doi.org/10.1128/mmbr.58.3.491-562.1994
43. Suhrbier, A. (2019). Rheumatic manifestations of chikungunya: emerging concepts and interventions. In *Nature Reviews Rheumatology* (Vol. 15, Issue 10). https://doi.org/10.1038/s41584-019-0276-9
44. Tang, J., Jose, J., Chipman, P., Zhang, W., Kuhn, R. J., & Baker, T. S. (2011).

Molecular links between the E2 envelope glycoprotein and nucleocapsid core in Sindbis virus. *Journal of Molecular Biology*, *414*(3). https://doi.org/10.1016/j.jmb.2011.09.045

45. Troost, B., Mulder, L. M., Diosa-Toro, M., van de Pol, D., Rodenhuis-Zybert, I. A., & Smit, J. M. (2020). Tomatidine, a natural steroidal alkaloid shows antiviral activity towards chikungunya virus in vitro. *Scientific Reports*, *10*(1). https://doi.org/10.1038/s41598-020-63397-7
46. Tsetsarkin, K. A., Vanlandingham, D. L., McGee, C. E., & Higgs, S. (2007). A single mutation in Chikungunya virus affects vector specificity and epidemic potential. *PLoS Pathogens*, *3*(12). https://doi.org/10.1371/journal.ppat.0030201
47. Varghese, F. S., Kaukinen, P., Gläsker, S., Bespalov, M., Hanski, L., Wennerberg, K., Kümmerer, B. M., & Ahola, T. (2016). Discovery of berberine, abamectin and ivermectin as antivirals against chikungunya and other alphaviruses. *Antiviral Research*, *126*. https://doi.org/10.1016/j.antiviral.2015.12.012
48. Volk, S. M., Chen, R., Tsetsarkin, K. A., Adams, A. P., Garcia, T. I., Sall, A. A., Nasar, F., Schuh, A. J., Holmes, E. C., Higgs, S., Maharaj, P. D., Brault, A. C., & Weaver, S. C. (2011). Genome-Scale Phylogenetic Analyses of Chikungunya Virus Reveal Independent Emergences of Recent Epidemics and Various Evolutionary Rates. *Journal of Virology*, *85*(11). https://doi.org/10.1128/jvi.00628-11
49. Voss, J. E., Vaney, M. C., Duquerroy, S., Vonrhein, C., Girard-Blanc, C., Crublet, E., Thompson, A., Bricogne, G., & Rey, F. A. (2010). Glycoprotein organization of Chikungunya virus particles revealed by X-ray crystallography. *Nature*, *468*(7324). https://doi.org/10.1038/nature09555
50. Vrouenraets, S. M. E., Wit, F. W. N. M., van Tongeren, J., & Lange, J. M. A. (2007). Efavirenz: A review. In *Expert Opinion on Pharmacotherapy* (Vol. 8, Issue 6). https://doi.org/10.1517/14656566.8.6.851

51. Wallace, A. C., Laskowski, R. A., & Thornton, J. M. (1995). Ligplot: A program to generate schematic diagrams of protein-ligand interactions. *Protein Engineering, Design and Selection*, *8*(2). https://doi.org/10.1093/protein/8.2.127

52. Zhang, M. Q., & Wilkinson, B. (2007). Drug discovery beyond the 'rule-of-five.' *Current Opinion in Biotechnology*, *18*(6), 478–488. https://doi.org/10.1016/J.COPBIO.2007.10.005

53. Zhang, W., Mukhopadhyay, S., Pletnev, S. V., Baker, T. S., Kuhn, R. J., & Rossmann, M. G. (2002). Placement of the Structural Proteins in Sindbis Virus. *Journal of Virology*, *76*(22). https://doi.org/10.1128/jvi.76.22.11645-11658.2002